Synthesis, Structure, and Properties of μ-Oxo-Bridged Fe^{III}_2 and Heterometallic Azide-Bridged $Fe^{III}_2Cu^{II}$ Complexes of a Picolinamide In-Plane Ligand

José M. Domínguez-Vera,*[a] José Suárez-Varela,[a] Ikram Ben Maimoun,[b] and Enrique Colacio*[a]

Keywords: Azides / Heterometallic complexes / Iron / Magnetic properties / Oxo ligands

A new μ-oxodiiron(III) complex $[\{Fe^{III}(bpc)(H_2O)\}_2O]$ (**1**) with the bis(picolinamide) N_4 in-plane ligand 4,5-dichloro-1,2-bis(pyridine-2-carboxamido)benzene (H_2bpc) has been prepared by the reaction of $[Fe(bpc)Cl(H_2O)]$ with a stoichiometric amount of cyanide, and characterized by X-ray structure analysis. The IR and UV/Vis spectroscopic results match well with those expected from the respective previously established spectro-structure correlation. Likewise, the temperature dependence of the magnetic susceptibility shows the existence of a strong antiferromagnetic coupling between the iron(III) centers [$S = 5/2$; with $J = -108.10(3)\ cm^{-1}$] that is consistent with the radial and angular overlap Weihe–Güdel model in μ-oxodiiron(III) complexes. Two heterometallic $Fe^{III}Cu^{II}Fe^{III}$ (**2**) and $Fe^{III}Ni^{II}Fe^{III}$ (**3**) complexes have been prepared from the reaction between $[Fe^{III}(bpc)(N_3)_2]$ and $[Cu(meso\text{-}CTH)]^{2+}$ or $[Ni(meso\text{-}CTH)]^{2+}$ (CTH = 5,7,7,12,14,14-hexamethyl-1,4,8,11-tetraazacyclotetradecane), respectively. The structure of **2** consists of heterometallic $Fe^{III}Cu^{II}Fe^{III}$ units formed by the simultaneous coordination of two $[Fe^{III}(bpc)(N_3)_2]$ units to the central $[Cu(meso\text{-}CTH)]$ units through a $\mu_{1,3}$-azide bridging ligand. However, the structure of **3** contains isolated $[Fe^{III}(bpc)(N_3)_2]^-$ and $[Ni(meso\text{-}CTH)]^{2+}$ ions. The treatment of the magnetic data of **2** revealed the existence of a small ferromagnetic interaction between Fe^{III} and Cu^{II} metal ions, with $J_{FeCu} = 3.24(7)\ cm^{-1}$. The existence of **2** opens up the possibility of obtaining, in a rational manner, azide-bridged heterometallic complexes starting from the block precursor $[Fe^{III}(bpc)(N_3)_2]^-$.

Introduction

Oxo-bridged diiron complexes have been extensively studied owing to the occurrence of the Fe–O–Fe fragment at the active sites of non-heme iron metalloproteins, such as hemerythrin,[1] ribonucleotide reductase,[2] or methane monooxygensase.[3] The synthetic, spectroscopic, and magnetic study of μ-oxodiiron complexes can provide a reference frame for these biological sites, and with this aim a great number of $(\mu\text{-oxo})L_2Fe_2$ complexes have been structurally characterized and their properties intensively studied.[4] In spite of this, the interest in preparing this kind of complexes remains because minor structural modifications in the L ligand or in the bridging region can generate drastic differences in their reactivity and properties, as is the case at the active site of metalloproteins.

One of the most commonly used strategies to prepare $(\mu\text{-oxo})L_2Fe_2$ complexes has been the hydrolysis, in a basic medium, of an in-plane ligand containing iron(III) complex. The ligand 4,5-dichloro-1,2-bis(pyridine-2-carboxamido)benzene (H_2bpc) is a good candidate for preparing this kind of diiron(III) complex since it is forced to occupy four in-plane nitrogen coordinative positions around an iron(III) ion. Monodentate ligands such as water, chloride, cyanide, azide, etc. can be bound in axial positions to generate six-coordinate distorted octahedral complexes $[Fe^{III}(bpc)X_2]$ and/or $[Fe^{III}(bpc)XY]$[5,6] (Scheme 1).

In this paper, we report on the synthesis, crystal structure, and magnetic properties of the μ-oxo dimer complex $[\{Fe^{III}(bpc)(H_2O)\}_2O]$ (**1**) and the heterometallic complexes $[\{Fe^{III}(bpc)(N_3)_2\}_2\{Cu(meso\text{-}CTH)\}]$ (**2**) and $[\{Fe^{III}(bpc)(N_3)_2\}_2\{Cu(meso\text{-}CTH)\}]$ (**3**). The former was prepared from the complex $[\{Fe^{III}(bpc)Cl(H_2O)]$, whereas **2** and **3** were prepared by the reaction between $[Fe^{III}(bpc)(N_3)_2]^-$ and $[Cu(meso\text{-}CTH)]^{2+}$ or $[Ni(meso\text{-}CTH)]^{2+}$ (CTH = 5,7,7,12,14,14-hexamethyl-1,4,8,11-tetraazacyclotetradecane), respectively. The existence of **2** suggests the possibility of preparing, in a rational manner, azide-bridged heterometallic complexes from the precursor $[Fe^{III}(bpc)(N_3)_2]^-$.

---

[a] Departamento de Química Inorgánica, Facultad de Ciencias,
Universidad de Granada,
18071 Granada, Spain
Fax: +34-958-248526
E-mail: ecolacio@ugr.es
[b] Department of Chemistry, Faculty of Sciences M'hannech,
University of Tetouan,
Morocco

DOI: 10.1002/ejic.200400911

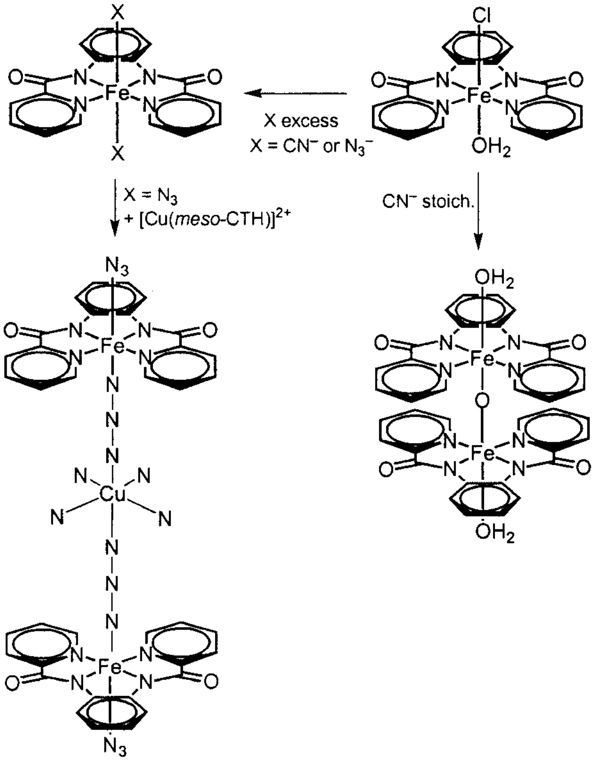

Scheme 1. Schematic preparation of the complexes.

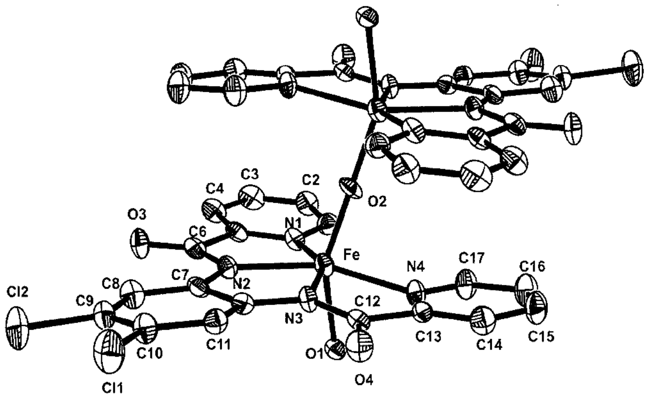

Figure 1. A perspective view of the structure of complex **1**. Hydrogen atoms and lattice water molecules have been omitted for clarity.

Table 1. Selected bond lengths [Å] and angles [°] for complex **1**.

N1–Fe	2.153(5)	N2–Fe	–
N3–Fe	2.086(5)	N4–Fe	–
O1–Fe	2.145(4)	O2–Fe	–
O2–Fe	1.7790(11)		–
Fe–O2–Fe	180.000(1)	O2–Fe–N2	105.29(15)
O2–Fe–N3	110.02(15)	N2–Fe–N3	77.7(2)
O2–Fe–O1	146.77(11)	N2–Fe–O1	99.61(18)
N3–Fe–O1	96.40(17)	O2–Fe–N1	86.09(15)
N2–Fe–N1	75.3(2)	N3–Fe–N1	151.5(2)
O1–Fe–N1	79.27(18)	O2–Fe–N4	87.32(14)
N2–Fe–N4	152.5(2)	N3–Fe–N4	75.0(2)
O1–Fe–N4	80.26(18)	N1–Fe–N4	130.8(2)

Results and Discussion

As previously reported, the complex [Fe^{III}(bpc)Cl(H_2O)] reacts with an excess of cyanide to produce the green complex [Fe^{III}(bpc)$(CN)_2$]$^-$.[6] However, when we carried out this reaction under stoichiometric conditions we obtained red crystals of the μ-oxodiiron(III) complex [{Fe^{III}(bpc)(H_2O)}$_2$O]·3H_2O (**1**). This suggests that the role of the cyanide salt in this reaction is as a base rather than as a ligand. In fact, the same complex [{Fe^{III}(bpc)(H_2O)}$_2$O] has previously been obtained using an inorganic base such as (Bu_4N)(OH) instead of cyanide,[7] although its structure was not reported. The molecular structure of **1** is shown in Figure 1, and selected bond lengths and angles are listed in Table 1.

The structure consists of μ-oxo dinuclear molecules in which the two iron atoms have a distorted octahedral geometry, with the four nitrogen atoms of the bis(picolinamidate) ligand in basal positions and two oxygen atoms in axial positions, one belonging to the μ-oxo bridge and another one to a water molecule. The tetradentate behavior of the ligand results in the formation of three five-membered rings around each iron atom. The Fe–N distances involving the pyridine nitrogen atoms N1 (2.154 Å) and N4 (2.167 Å) are significantly longer than those for the amide nitrogen atoms N2 (2.059 Å) and N3 (2.086 Å). Similar bond-length patterns have been observed for other related iron(III) complexes.[8] The central oxygen atom of the Fe–O–Fe fragment lies on an inversion center, with an Fe–O–Fe angle of 180° and an Fe–Fe distance of 3.558 Å, which is typical of a monobridged Fe–O–Fe linear core.[4] The μ-oxo–Fe and Fe–O(water) distances of 1.779 and 2.145 Å are similar to those previously reported for related iron(III) complexes.[9] Within the dimer, essentially planar Fe(bpc) units stack in such a way that the Cl–Cl interactions are minimized, whereas extensive π-π interactions remain in the structure. As a result, the Fe(bpc) fragments are shifted with respect to each other and the angle formed between the μ-oxo oxygen atom O2 and the mean FeN_4 coordination plane increases from 90° to 98°.

The UV/Vis and IR spectroscopic properties of the μ-oxodiiron(III) system have been analyzed in detail, allowing the establishment of nice correlations between structural and spectroscopic data. The UV/Vis spectrum of **1** shows a unique band at 355 nm in the so-called "oxo dimer region", which is consistent with the linearity of the Fe–O–Fe unit found in the present complex.[4] The IR spectrum shows two bands at 837 and 442 cm^{-1}, attributed to the asymmetric and symmetric Fe–O–Fe vibrations, respectively, which usually are in the range 885–725 and 540–380 cm^{-1}.[4] As has been previously established, the location of these two bands depends strongly on the Fe–O–Fe angle: the lower the angle, the less energetic the asymmetric and more energetic the symmetric Fe–O–Fe vibrations observed.[4,10] Therefore, the two bands found for **1** at 837 and 442 cm^{-1} match well with the linearity of the Fe–O–Fe bridge.

As indicated elsewhere, complex **1** can also be obtained from the reaction between [Fe^{III}(bpc)Cl(H_2O)] and cyanide in a 1:1 ratio (Scheme 1). When an excess of cyanide is used, two cyanide ligands coordinate to the iron ion to give the complex $[Fe^{III}(bpc)(CN)_2]^-$. Other related $[Fe^{III}(bpc)(X)_2]$ complexes (X = azide, pyridine, etc.) can also be prepared in the presence of an excess of the X ligand (Scheme 1).[5] We explored the possibility of making use of this kind of complex $[Fe^{III}(bpc)(X)_2]$ ($X = CN^-$ or N_3^-) as a precursor of polymetallic complexes in a similar way to that used by Holm[11] and Murray et al.,[12] which is by the coordination of the axial X ligands to metal complexes with empty coordination sites. We observed in the course of this research that the reaction between $[Fe^{III}(bpc)(CN)_2]^-$ and [M(*meso*-CTH)]$(ClO_4)_2$ did not give rise to the expected heterometallic complex but to the μ-oxo dimer **1**. However, from the reaction between $Na[Fe^{III}(bpc)(N_3)_2]$ and [M(*meso*-CTH)]$(ClO_4)_2$ (M = Cu^{II}, Ni^{II}), we succeeded in obtaining the heterometallic complexes $[\{Fe^{III}(bpc)(N_3)_2\}_2$\{Cu(*meso*-CTH)\}] (**2**) and $[\{Fe^{III}(bpc)(N_3)_2\}_2$\{Ni(*meso*-CTH)\}] (**3**), whose structures were solved by X-ray diffraction.

The molecular structure of complex **2** is shown in Figure 2, and selected bond lengths and angles are listed in Table 2.

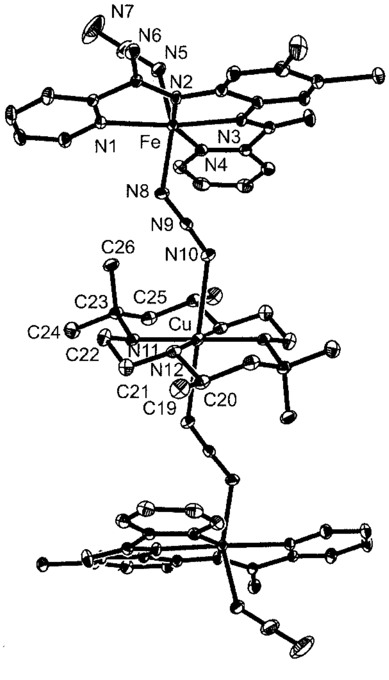

Figure 2. A perspective view of the structure of complex **2**. Hydrogen atoms and the lattice water molecule have been omitted for clarity.

The structure consists of centrosymmetric heterometallic $Fe^{III}Cu^{II}Fe^{III}$ complexes, which are formed by the simultaneous coordination of two $[Fe^{III}(bpc)(N_3)_2]^-$ anions to the central [Cu(*meso*-CTH)]$^{2+}$ cation through a single end-to-end azide bridging ligand. The inversion center is located at the Cu^{II} ion and the Fe–Cu distance is 6.43 Å. The ligand environment around the central Cu^{II} ion can be described as a distorted octahedron. The four nitrogen atoms of the CTH ligand are bound in equatorial positions with typical Cu–N distances of about 2 Å, whereas the two azide ligands occupy the axial positions at longer distances of 2.597 Å, giving rise to a *trans* arrangement with a Cu–N10–N9 bond angle of 138.7°. The coordination geometry of the terminal Fe^{III} ions is close to octahedral, with structural parameters in the Fe(bpc) fragment close to those observed in **1** and other related complexes,[5,6] and with $Fe–N_{azide}$ distances of about 2.02 Å. The bond angles Fe–N8–N9 and Fe–N5–N6 are 129.3° and 130.5°. As usual, both the non-bridging and the azide-bridging ligands are practically linear, with values of 176.9(6)° and 174.3(5)°, respectively.

Table 2. Selected bond lengths [Å] and angles [°] for complex **2**.

Cu–N12	2.020(3)	Cu–N11	2.053(2)
N3–Fe	2.050(2)	N4–Fe	–
N1–Fe	2.211(2)	N2–Fe	–
Fe–N5	2.017(3)	Fe–N8	2.028(2)
N12–Cu–N11	94.13(10)	N5–Fe–N8	148.90(12)
N5–Fe–N2	102.43(11)	N8–Fe–N2	102.04(10)
N5–Fe–N3	100.89(11)	N8–Fe–N3	102.75(11)
N2–Fe–N3	77.94(9)	N5–Fe–N4	85.63(10)
N8–Fe–N4	80.83(10)	N2–Fe–N4	153.72(9)
N3–Fe–N4	75.97(9)	N5–Fe–N1	84.57(10)
N8–Fe–N1	83.06(10)	N2–Fe–N1	75.95(9)
N3–Fe–N1	153.88(9)	N4–Fe–N1	130.11(9)
N6–N5–Fe	130.5(3)	N10–N9–N8	–
N9–N8–Fe	129.3(2)	N7–N6–N5	–

However, when we tried to extend this strategy to obtain the heterometallic $Fe^{III}Ni^{II}Fe^{III}$ complex, by treating $Na[Fe^{III}(bpc)(N_3)_2]$ with [Ni(*meso*-CTH)]$(ClO_4)_2$, we obtained the complex $[\{Fe^{III}(bpc)(N_3)_2\}_2$\{Ni(*meso*-CTH)\}], whose structure consists of isolated $[Fe^{III}(bpc)(N_3)_2]^-$ and [Ni(*meso*-CTH)]$^{2+}$ ions (Figure 3) with an Ni–N10 distance of 3.453 Å. Selected bond lengths and angles are listed in Table 3. The bond lengths and angles in both ionic units are close to those found in **2** and other analogous compounds

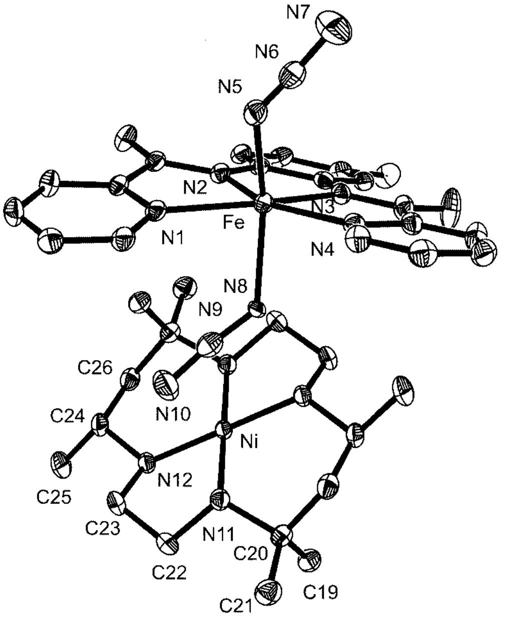

Figure 3. A perspective view of the structure of complex **3**. Hydrogen atoms have been omitted for clarity.

Magnetic Properties

The temperature dependence of χT per Fe for **1** in the range 298–2 K is shown in Figure 4. The χT product de-

Table 3. Selected bond lengths [Å] and angles [°] for complex **3**.

N1–Fe	2.171(3)	N8–Fe	–
N5–Fe	2.040(4)	N2–Fe	–
N3–Fe	2.055(3)	N4–Fe	–
Ni–N11	1.942(4)	Ni–N12	1.961(3)
N9–N8–Fe	129.9(3)	N8–N9–N10	–
N6–N5–Fe	131.5(4)	N5–N6–N7	–
N5–Fe–N2	98.55(15)	N5–Fe–N3	108.21(15)
N2–Fe–N3	77.21(12)	N5–Fe–N8	149.72(15)
N2–Fe–N8	103.89(13)	N3–Fe–N8	96.50(12)
N5–Fe–N1	82.71(14)	N2–Fe–N1	76.64(12)
N3–Fe–N1	152.90(13)	N8–Fe–N1	82.98(11)
N5–Fe–N4	85.74(14)	N2–Fe–N4	153.37(12)
N3–Fe–N4	76.50(13)	N8–Fe–N4	83.25(12)
N1–Fe–N4	129.96(12)	N11–Ni–N12	93.50(14)

creases with the temperature, as expected for strongly antiferromagnetically coupled $S = 5/2$ pairs. The experimental data were analyzed using the van Vleck equation with $H = -2JS_1 \cdot S_2$ ($S_1 = S_2 = 5/2$). Because the χT plateau value at low temperature is not zero, the existence of a monomer impurity (p) was taken into account, which is a common feature of μ-oxodiiron(III) systems.

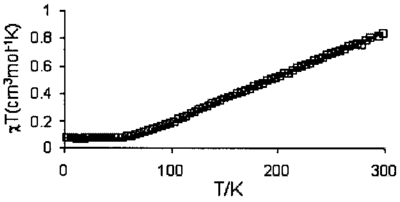

Figure 4. Temperature dependence of $\chi_M T$ for **1**. Solid lines represent the best data fit.

A very good fit of the data was obtained for $J = -108.1$ cm^{-1}, $p = 1.5\%$, and g fixed to 2.00. The J value of -108.1 cm^{-1} compares well with that calculated by using the angular and radial overlap model of Weihe and Gudel ($J = -106.1$ cm^{-1})[13] for μ-oxodiiron(III) complexes. In this model, the Fe–O–Fe angle and the average Fe–O distances are correlated with J. However, by using the empirical correlation obtained by Lippard,[14] which ignores the angular dependence and only includes the Fe–O distance, a J value of -92 cm^{-1} is obtained.

The magnetic susceptibility data for a polycrystalline sample of **2** were measured in the temperature range 2–300 K (Figure 5).

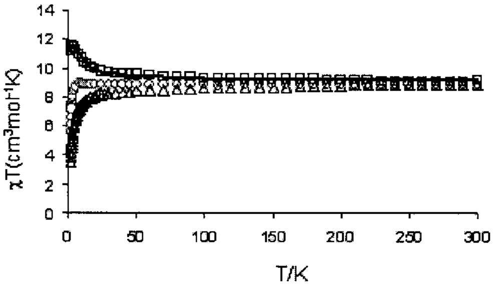

Figure 5. Temperature dependence of $\chi_M T$ for **2** (circles) and NBu$_4$-[Fe(L)(N$_3$)$_2$] (triangles). Temperature dependence of of $\chi_M T$ for **2** once the ZFS corresponding to two Fe^{III} ions has been removed (squares). The solid lines represent the best data fit to the theoretical model.

At room temperature, the $\chi_M T$ product (χ_M is the magnetic susceptibility per Fe$_2$Cu trinuclear molecule) is 8.83 cm^{3}mol^{-1}K, which is close to the calculated value of 9.125 for an uncoupled system with two high-spin Fe^{III} ions ($S = 5/2$) and one Cu^{II} ion ($S = 1/2$), assuming an average g value of 2.0. As the temperature is lowered, $\chi_M T$ remains almost constant until about 12 K, then increases very slightly and finally decreases sharply upon cooling to 2 K. If the two iron(III) and the copper(II) ions were magnetically isolated, at low temperature the $\chi_M T$ product should decrease with the temperature in a similar manner as in the mononuclear complex Bu$_4$N[Fe(L)(N$_3$)$_2$]. However, as can be observed in Figure 5, the decrease in $\chi_M T$ for Bu$_4$N-[Fe(L)(N$_3$)$_2$] begins at higher temperatures, which might suggest the existence of a weak ferromagnetic interaction between the Fe^{III} and Cu^{II} ions in **2** similar to that observed for the closely related complex [Cu(cyclam){Fe(L)-(N$_3$)$_2$}$_2$].[15] This fact prompted us to analyze in detail the experimental magnetic data of **2** in order to determine whether or not a weak ferromagnetic interaction exists. Because the sharp decrease in $\chi_M T$ due to local anisotropy of the Fe^{III} ions might mask the increase in $\chi_M T$ caused by a hypothetical ferromagnetic interaction, we removed the contribution of the decrease in $\chi_M T$ for two Fe^{III} ions with a similar coordination environment to that exhibited by the Fe^{III} ions in **2** from the experimental magnetic data. In this regard, we used the magnetic data of the complex Bu$_4$N-[Fe(L)(N$_3$)$_2$]. As result of this, a different $\chi_M T$ vs. T dependence was obtained. As can be observed in Figure 5, as the temperature is lowered $\chi_M T$ remains almost constant until around 100 K, then increases to reach a maximum with a value of 11.55 cm^{3}mol^{-1}K at 3 K. Such a magnetic behavior confirms our hypothesis of the existence of a ferromagnetic coupling between the central Cu^{II} ion and the terminal Fe^{III} ions. The modified data were fitted to the equation for three linearly coupled spins derived from the spin Hamiltonian $H = -J(S_{Fe1} \cdot S_{Cu} + S_{Fe2} \cdot S_{Cu})$. The remote coupling constant, J_{FeFe}, between terminal Fe^{III} ions separated by a distance higher than 12 Å, was assumed to be zero. It was necessary to include a constant, θ, to fit the decrease of $\chi_M T$ at very low temperature. The expression used was $\chi = (C/\mathrm{T} - \theta) f(J_{FeCu}, T)$ where $C = Ng^2\mu_B{}^2/k$ and $f(J_{FeCu}, T)$ is derived from the theoretical equation. The best parameters obtained with this model were $J_{FeCu} = 3.24(7)$ cm^{-1}, $g_{av} = 2.001(1)$, and $\theta = -0.90(2)$. The ferromagnetic coupling observed can be explained in terms of orbital considerations. The magnetic orbital of the copper(II) atom is of the type $d_{x^2-y^2}$ − the x and y axes being defined by the short Cu–N(cyclam) bonds − with a very low spin density on the axial positions (z axis), which are filled by the N atoms of the bridging azide ligands. This leads to a negligible overlap ($J_{AF} \approx 0$) and to a weak ferromagnetic interaction ($J \approx J_F$). The large Cu–N$_{azide}$ distance of 2.597 Å also accounts for the weakness of the magnetic coupling observed. Nevertheless, the value of J should be taken with caution because of the crude procedure followed in its estimation.

Experimental Section

Synthesis: The H_2bpc ligand[5] and the complexes [Fe^{III}(bpc)Cl(H_2O)]·H_2O, Na[Fe^{III}(bpc)(N_3)$_2$], Na[Fe^{III}(bpc)(CN)$_2$],[6] [Cu(*meso*-CTH)](ClO_4)$_2$. and [Ni(*meso*-CTH)](ClO_4)$_2$[16] were prepared as previously reported.

Caution*: Perchlorate and cyanide salts are potentially explosive and poisonous, respectively, and should be used in small quantities. Due care must be taken when handling perchlorate and cyanide salts.*

[{Fe^{III}(bpc)(H_2O)}$_2$O]·3H_2O (1): A methanol suspension (50 mL) of [Fe^{III}(bpc)Cl(H_2O)]·H_2O (0.512 g, 1.0 mmol) containing a stoichiometric amount of NaCN (49 mg) was stirred at room temperature for 1 h. The resultant red solution was kept at room temperature to produce orange crystals, which were filtered and air-dried. Yield: 68%. $C_{36}H_{32}Cl_4Fe_2N_8O_{11}$: calcd. C 42.94, H 3.18, N 11.13; found C 43.02, H 3.28, N 11.19.

[{Fe^{III}(bpc)(N_3)$_2$}$_2${Cu(*meso*-CTH)}]·2H_2O (2): A methanol suspension (30 mL) of [Fe(L)Cl(H_2O)]·H_2O (41 mg, 0.08 mmol) and NaN_3 (10.4 mg, 0.16 mmol) was stirred until the formation of a clear green solution. The solution was then filtered to remove any insoluble material. A methanol solution (20 mL) of [Cu(cyclam)(ClO_4)$_2$] (22 mg, 0.04 mmol) was slowly added to the filtrate, after which the mixture was stirred for 15 min. Dark-green crystals were obtained from the filtrate by slow concentration at room temperature for 2 d. Yield: 65% based on copper. IR (KBr): ν(N–N–N) = 2073 and 2050 cm^{-1}. $C_{52}H_{60}Cl_4CuFe_2N_{24}O_6$: calcd. C 43.67, H 3.95, N 23.50; found C 43.56, H 4.15, N 23.54.

[{Fe^{III}(bpc)(N_3)$_2$}$_2${Ni(*meso*-CTH)}] (3): This compound was obtained in a similar way as **2** using [Ni(*meso*-CTH)](ClO_4)$_2$ instead of [Cu(*meso*-CTH)](ClO_4)$_2$. Yield: 59%. IR (KBr): ν(N–N–N) = 2050 cm^{-1}. $C_{52}H_{56}Cl_4Fe_2N_{24}NiO_4$: calcd. C 44.78, H 4.02, N 24.11; found C 44.87, H 3.91, N 23.96.

Measurements: The IR spectra of powdered samples were recorded with a ThermoNicolet IR200FTIR and the UV/Vis spectra of **1** with a Thermospectronic UV300 spectrophotometer against a reference solution containing appropriate amounts of the ligand bpc. Variable-temperature (1.9–300 K) magnetic susceptibility measurements on polycrystalline samples were carried out with a Quantum Design Squid operating at different magnetic fields. Experimental susceptibilities were corrected for diamagnetism and magnetization of the sample holder.

X-ray Diffraction: The unit-cell parameters were determined and the data collected at room temperature with a Siemens STOE STADI4 four-circle diffractometer. The data were corrected for Lorentz polarization effects and for dispersion, and an empirical absorption correction was applied. The structures were solved by direct methods using SHELXS-97[17] and refined (full-matrix least squares on F^2) with all non-hydrogen atoms refined anisotropically with SHELXL97 and WINGX.[18] All hydrogen atoms were geometrically fixed and allowed to ride on the attached atoms. The crystal and refinement details for compounds **1**–**3** are listed in Table 4. CCDC-253934 to -253936 (**1**–**3**, respectively) contain the supplementary crystallographic data for this paper. These data can be obtained free of charge from The Cambridge Crystallographic Data Centre via www.ccdc.cam.ac.uk/data_request/cif.

Acknowledgments

This work was supported by the Spanish Ministry of Science and Education (Project BQU2001-3221) and the Junta de Andalucia. I. B. M. thanks the Spanish Agency of International Cooperation (AECI) for a predoctoral grant.

---

[1] R. E. Stenkamp, *Chem. Rev.* **1994**, *94*, 715–726.

[2] J. Stubbe, W. A. Donk, *Chem. Biol.* **1995**, *2*, 793–801.

[3] C. Rosenzweig, P. Nordlund, P. M. Takahara, C. A. Frederick, S. J. Lippard, *Chem. Biol.* **1995**, *2*, 409–418.

[4] D. M. Kurtz, Jr., *Chem. Rev.* **1990**, *90*, 585.

[5] D. J. Barnés, R. L. Chapman, R. S. Vagg, E. C. Watton, *J. Chem. Eng. Data* **1978**, *23*, 349–350.

[6] a) M. Ray, R. Mukherjee, J. F. Richardson, R. M. Buchanan, *J. Chem. Soc., Dalton Trans.* **1993**, 2451–2457; b) S. K. Dutta, U. Beckmann, E. Bill, T. Weyhermüller, K. Wieghardt, *Inorg. Chem.* **2000**, *39*, 3355–3364.

[7] A. K. Patra, R. Mukherkee, *Polyhedron* **1999**, *18*, 1317–1322.

[8] E. Balogh-Hergovich, G. Speier, M. Réglier, M. Giorgi, E. Kuzmann, A. Vértes, *Eur. J. Inorg. Chem.* **2003**, 1735–1740.

[9] P. C. Junk, B. J. McCool, B. Moubaraki, K. S. Murray, L. Spiccia, J. D. Cashion, J. W. Steed, *J. Chem. Soc., Dalton Trans.* **2002**, 1024–1029.

[10] R. E. Norman, R. C. Holz. S. Ménage, C. J. O'Connor, J. H. Zhang, L. Que, Jr., *Inorg. Chem.* **1990**, *29*, 4629–4630.

[11] a) M. J. Scott, R. H. Holm, *J. Am. Chem. Soc.* **1994**, *116*, 11357–67; b) M. J. Scott, C. S. Lee, R. H. Holm, *Inorg. Chem.* **1994**, *33*, 4651–62.

Table 4. Crystal data for complexes **1**–**3**.

	1	2	3
Empirical formula	$C_{36}H_{32}N_8O_{11}Fe_2Cl_4$	$C_{52}H_{60}N_{24}O_6Fe_2CuCl_4$	$C_{52}H_{56}N_{24}O_4Fe_2NiCl_4$
Formula mass	1006.16	1434.24	1393.42
Crystal system	monoclinic	monoclinic	monoclinic
Space group	$P12_1/n$ (no. 1)	$P12_1/n$ (no. 1)	$P12_1/c$ (no. 1)
a [Å]	12.2156(48)	11.9165(5)	10.0924(7)
b [Å]	9.6771(37)	20.9026(9)	13.8648(9)
c [Å]	17.9909(69)	13.2751(6)	20.7871(13)
α [°]	90	90	90
β [°]	92.173(8)	108.434(1)	96.374(1)
γ [°]	90	90	90
V [Å^3]	2125.20(16)	3136.97(11)	2890.74(5)
Z	2	3	2
μ [mm^{-1}]	0.995	1.032	1.072
Goodness-of-fit	0.734	1.132	1.035
Refl. collected/unique	9404/3040	36267/7203	18191/6580
Final R indices	R_1 = 0.049	R_1 = 0.051	R_1 = 0.063
[$I > 2\sigma(I)$]	wR_2 = 0.081	wR_2 = 0.118	wR_2 = 0.154

[12] R. J. Parker, K. D. Lu, S. R. Batten, B. Moubaraki, K. S. Murray, L. Spiccia, J. D. Cashion, A. D. Rae, A. C. Willis, *J. Chem. Soc., Dalton Trans.* **2002**, 3723–3730.
[13] H. Weihe, H. Gudel, *J. Am. Chem. Soc.* **1997**, *119*, 6539.
[14] S. M. Gorun, S. J. Lippard, *Inorg. Chem.* **1991**, *30*, 1625.
[15] E. Colacio, J.-P. Costes, J. M. Domínguez-Vera, I. B. Maimoun, J. Suárez-Varela, *Chem. Commun.* **2005**, 534–536.
[16] N. F. Curtis, D. A. Swann, T. N. Waters, *J. Chem. Soc., Dalton Trans.* **1973**, 1963.
[17] G. M. Sheldrick, *SHELXLS-97, Program for Solution of Crystal Structure*, University of Göttingen, Germany, **1997**.
[18] a) G. M. Sheldrick, *SHELXL-97, a computer program for refinement of crystal structures*, University of Göttingen, Germany, **1997**; b) L. J. Farrugia, *J. Appl. Crystallogr.* **1999**, *32*, 837.

Received: October 28, 2004